Advanced Journal of Chemistry-Section A

Journal homepage: www.ajchem-a.com

Original Research Article

Synthesis, Antibacterial, Antifungal and DFT Studies on Structural, Electronic and Chemical Reactivity of (*E*)-7-((1*H*-Indol-3-yl)methylene)-1,2,6,7-tetrahydro-8*H*-indeno[5,4-*b*]furan-8-one

Vishnu Ashok Adole*

PG Department of Chemistry, Mahatma Gandhi Vidyamandir's Arts, Science and Commerce College, Manmad, Taluka-Nandgaon, District- Nashik, India-423104

ARTICLE INFO

Article history

Submitted: 20 March 2021
Revised: 09 April 2021
Accepted: 18 April 2021
Available online: 19 April 2021
Manuscript ID: AJCA-2103-1250

DOI: 10.22034/AJCA.2021.278047.1250

KEYWORDS

6-311G(d,p)
Computational
FMO
Antimicrobial
MESP

ABSTRACT

The present study deals with the theoretical investigation of structural, molecular, electronic, and chemical reactivity details of (*E*)-7-((1*H*-indol-3-yl)methylene)-1,2,6,7-tetrahydro-8*H*-indeno[5,4-*b*]furan-8-one (ITHF). The **ITHF** molecule is characterized by proton nuclear magnetic resonance (^{1}H NMR) and carbon nuclear magnetic resonance (^{13}C NMR) spectral techniques. The Becke-3-Lee-Yang-Parr functional (B3LYP) level of theory at the 6-311G(d,p) basis set was used for the density functional theory (DFT) investigation. Bond lengths were predicted from the optimized molecular structure, and the physical and chemical properties of the molecules were inferred as a consequence. The HOMO and LUMO are computed and their energies were established. The calculated HOMO-LUMO energy gap is 3.67 eV indicating inevitable electron transfer phenomenon within the **ITHF** molecule. Amongst all carbon atoms, the C6 carbon as more positive and C21 as more negative carbon atoms. The molecular electrostatic surface potential revealed that the negative electrostatic potential is present over oxygen atoms and the positive, on the other hand, is located over two aromatic rings' hydrogen atoms in the **ITHF** molecule. Importantly, the **ITHF** compound were evaluated for antibacterial activities against two Gram positive bacteria namely *Bacillus subtilis* and *Staphylococcus aureus* and two Gram negative bacteria namely *Escherichia coli* and *Proteus vulgaris* and two fungal agents namely *Aspergillus niger* and *Candida albicans*. The **ITHF** compound was found to show good antimicrobial action.

* Corresponding author: Adole, Vishnu Ashok
✉ E-mail: vishnuadole86@gmail.com

GRAPHICAL ABSTRACT

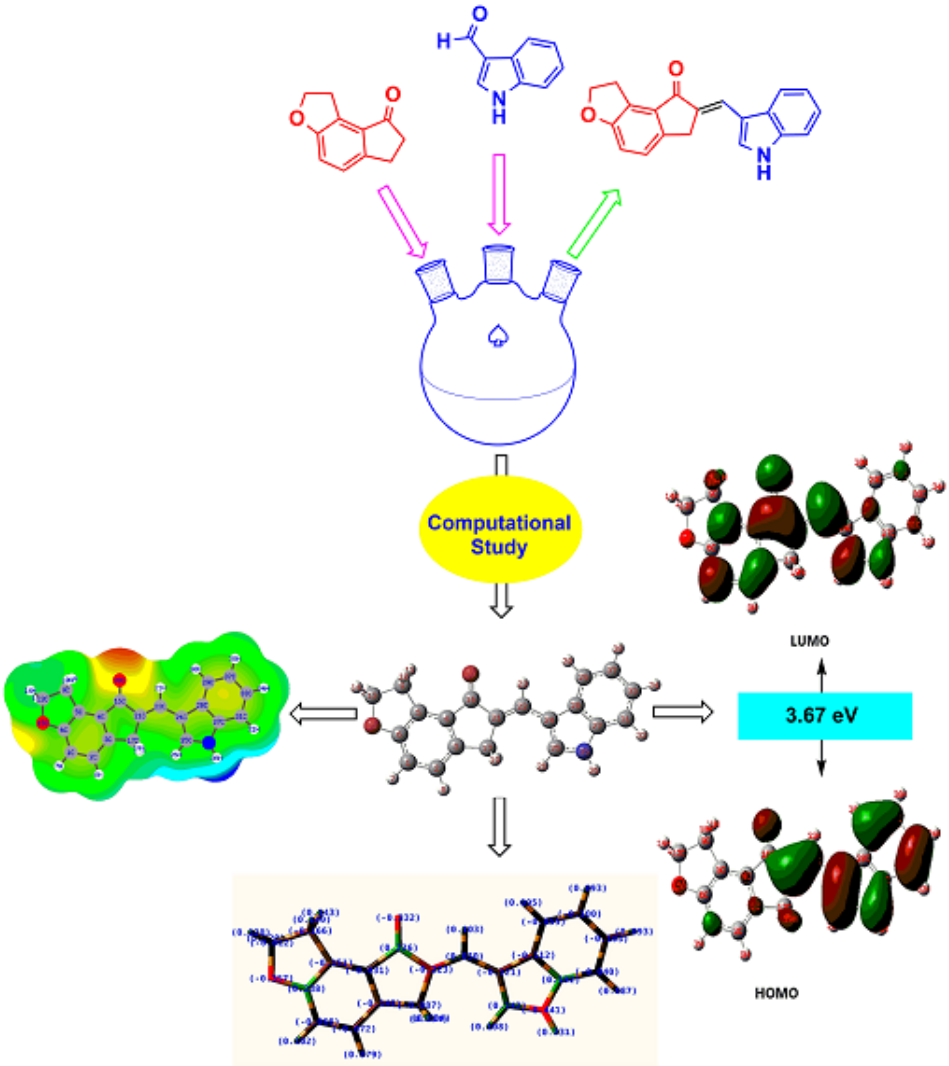

Introduction

Indole is a privileged s heterocyclic framework in view of its incorporation with proteins as amino acid tryptophan. Indole is a planar bicyclic compound with a benzene and pyrrole ring fused together. Since medicinal compounds have an indole center, they are a special heterocyclic structure with a wide variety of biological properties [1-4]. The astonishing biological properties of heterocyclic compounds containing indole nucleus are antimicrobial [5], antitubercular [6], anticonvulsant [7], anti-inflammatory [8], analgesic [9], anticancer [10], insecticidal activity [11], antioxidant [12], antiviral [13], antidepressant [14], and antihistaminic [15]. Likewise, indanones appear to be a most promising lead for drug development [16-20].

Theoretical chemistry has advanced and DFT calculations are considered as valuable tool for predicting the structural, electronic, and spectral properties of the molecules [21-24]. Importantly, DFT computations offer a wealth of knowledge about the molecules' spectroscopic and quantum chemical parameters, allowing researchers to investigate their chemical behaviour [25-31]. DFT techniques have also been used to study UV-visible, NMR, and Raman spectroscopic examinations [32-34]. Theoretical calculations

using DFT has been used to asses various structural, molecular and spectral properties 2,3-dihydrobenzofuran derivatives [35], 5,6-diaroylisoindoline-1,3-dione [36] , morphonium formate and acetate Ionic liquid salts [37] 2,3-dihydrobenzofuran linked indanones [38], 2-(3-bromophenyl)-4-(4-bromophenyl)-2,3-dihydro-1*H*-1,5-benzodiazepine [39], (*E*)-3-(4-chlorophenyl)-1-(2-hydroxyphenyl)prop-2-en-1-one [40], ethyl 4-(4-isopropylphenyl)-6-methyl-2-oxo-1,2,3,4-tetrahydropyrimidine-5-carboxylate [41], 5-(4-chlorophenyl)-3-(3,4-dimethoxyphenyl)-1-phenyl-4,5-dihydro-1*H*-pyrzole [42], (*E*)-1-(2,3-dihydrobenzo[*b*][1,4]dioxin-6-yl)-3-(3,4,5-trimethoxyphenyl)prop-2-en-1one [43], dihydropyrimidinones [44], (2*E*)-3-(2,6-dichlorophenyl)-1-(4-fluoro)-prop-2-en-1-one [45], and ethyl-4-(3,4-dimethoxyphenyl)-6-methyl-2-oxo-1,2,3,4-tetrahydropyrimidine-5-carboxylate [46]. The efficient synthesis methods were found to speed up the rate of reaction and thereby follow the principles of green chemistry [47-53].

The DFT method with the B3LYP functional is proved to be one of the best computational strategies to predict molecular properties [54-62]. Using the B3LYP functional with a 6-311G(d,p) basis set, the great deal of agreement between theoretical and experimental results can be obtained [21, 22]. In light of all of the above, I would like to present a DFT analysis on the structural, mechanical, and chemical reactivity of (*E*)-7-((1*H*-indol-3-yl)methylene)-1,2,6,7-tetrahydro-8*H*-indeno[5,4-*b*]furan-8-one in this paper. The usefulness of DFT on molecular structure, bond length, bond angle, and Mulliken atomic charges has been explored in the flow study. The DFT technique was used to analyse essential parameters such as total energy, HOMO-LUMO energies, charge distribution, thermodynamic properties, and so on. This is the first article on the synthesis and DFT investigation of the title compound.

Experimental

General Remarks

The high-purity chemicals were purchased from the Sigma laboratory in Nashik. The chemicals were used exactly as they were obtained, with no further purification needed. The melting point was measured in an uncorrected open capillary system. A sophisticated multinuclear FT NMR Spectrometer model Advance-II (Bruker) was used to record ^{1}H and ^{13}C NMR spectra with a ^{1}H frequency of 500 MHz and ^{13}C frequency 126 MHz using DMSO-d6 as solvent. The reaction was monitored by thin-layer chromatography using aluminium sheets with silica gel 60 F254 (Merck).

Experimental Procedure for the Synthesis ITHF

A mixture of 1,2,6,7-tetrahydro-8*H*-indeno[5,4-*b*]furan-8-one (8 mmol) and 1*H*-indole-3-carbaldehyde (10 mmol) was mixed in 5 mL ethanol taken in a conical flask. To this mixture 2 mL 20 % NaOH was added. The resulting alkaline mixture was stirred on a magnetic stirrer at room temperature until the formation of the desired product (checked by TLC). The crude product was transferred into a beaker containing crushed ice, stirred, acidified by dilute HCl filtered, dried naturally, and recrystallized using hot ethanol to furnish pure yellow solid (Scheme 1).

Scheme 1. Synthesis of ITHF molecule

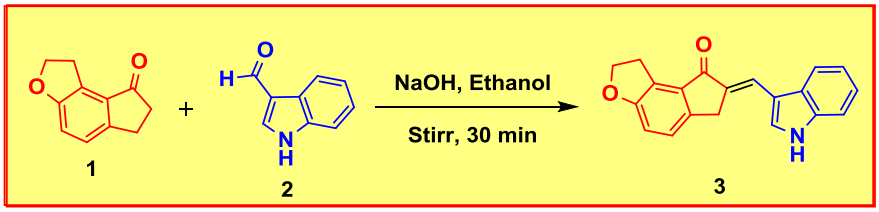

Computational Details

The Gaussian 03 W programme was used to perform all calculations [63]. DFT method with B3LYP functional was used for the theoretical simulations [64]. The title compound's geometry optimization and corresponding energy were determined using a 6-311G(d,p) base set and C1 point group symmetry. As a result, the optimum geometrical parameters, energy, atomic charges, dipole moment, were theoretically determined. In light of the optimised structure, the Mulliken atomic charges, molecular electrostatic potential surface, electronic properties such as HOMO–LUMO energies, and dipole moment were also investigated.

Antimicrobial Screening

The agar diffusion method was used to access the antimicrobial activities [65]. Chloramphenicol was used as a standard for antibacterial evaluation and Amphotericin-B for antifungal screening. The antibacterial screening was performed against *Escherichia coli*, *Proteus vulgaris*, *Staphylococcus aureus* and *Bacillus subtilis* while the antifungal screening was performed against *Aspergillus niger*, and *Candida albicans*.

Results and Discussion

Spectral Analysis of ITHF

The ^{1}H NMR spectrum predicts the types and total number of hydrogen atoms in the molecule. There are total of ten types of protons in the title molecule and therefore has furnished ten signals in the ^{1}H NMR spectrum. The NH group signal is located at 12.05 δ as broad singlet. The two proton present in benzene ring are ortho coupled with J = 7.1 Hz. All other signals are correctly matched with the structure of the **ITHF** molecule. The ^{13}C NMR spectrum predicts types of carbons atoms in the molecule and therefore one can anticipate the skeleton of the molecule. There are total of 20 types of carbons that have displayed 20 signals in the ^{13}C NMR spectrum affirming the structure. The signal at 193.23 δ is due to the carbonyl carbon of ketone group.

Spectral Data of the ITHF

^{1}H NMR (500 MHz, DMSO) δ 12.05 (s, 1H), 7.97 (m, 1H), 7.87 (d, J = 7.7 Hz, 1H), 7.84 (d, J = 2.1 Hz, 1H), 7.51 – 7.48 (m, 1H), 7.36 (d, J = 8.1 Hz, 1H), 7.24 – 7.20 (m, 1H), 7.08 (d, J = 8.1 Hz, 1H), 4.63 (t, J = 8.8 Hz, 2H), 3.91 – 3.87 (m, 2H), 3.46 (t, J = 8.8 Hz, 2H). ^{13}C NMR (126 MHz, DMSO) δ 193.23, 160.35, 141.10, 136.58, 135.59, 130.95, 129.35, 127.95, 125.73, 124.92, 124.31, 123.07, 121.14, 118.63, 114.98, 112.67, 112.10, 72.34, 32.72, 28.42.

Computational study

Molecular Structure Study

Figure 1 shows the optimised molecular structure of the title molecule. Figure 2 illustrates the geometrical viewpoints around various dimensions (A, B, and C Cartesian axes). The optimised molecular geometry reveals a lot about the spatial orientation of different atoms in a molecule. From optimized molecular structures, it tends to be handily observed that the **ITHF** molecule possesses C1 point group

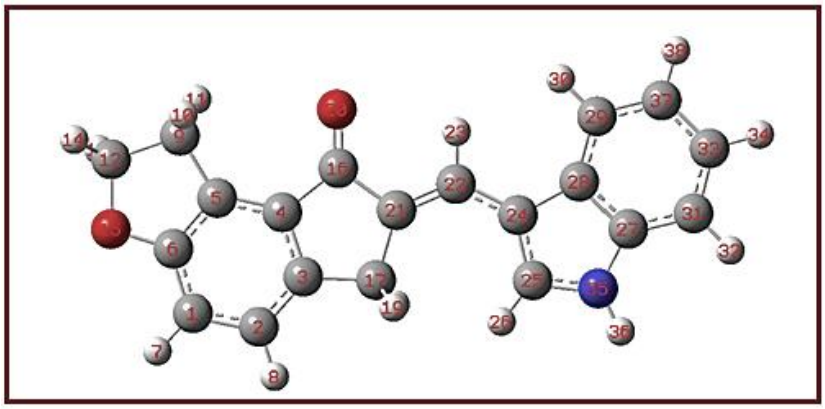

Figure 1. Optimized molecular structure of ITHF molecule

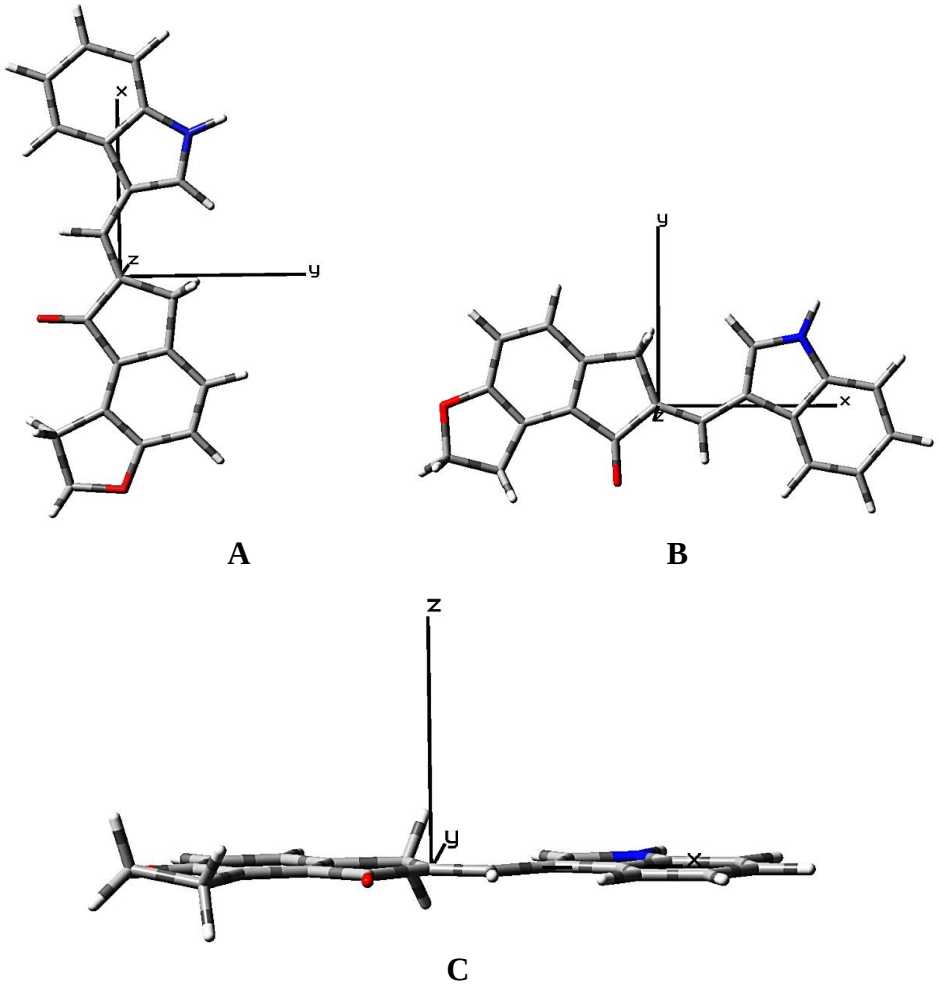

Figure 2. Molecular structures of ITHF molecule along Cartesian axes

symmetry due to the overall asymmetry of the molecule. Moreover, it is additionally apparent that it contains a non-planar dihydrofuran ring. The non-planarity of dihydrofuran can be ascribed to the CH_2 group (adjacent to an oxygen atom) which is either above or beneath the plane.

It can likewise be seen that the remaining skeleton is in immaculate planar position and hence can have broadened conjugation. This data is a lot of value for the assurance of different spectroscopic elements. The optimized geometrical parameters bond lengths and bond angles are presented in Table 1 and Table 2 respectively. The longest and the shortest aromatic (benzene ring) double bonds are C33-C37 (1.4072 Å) and C29-C37 (1.3869 Å) respectively. The C16-O20 bond length is 1.2207 Å and the C21-C22 is 1.3489 Å. The N35-H36 is 1.0064 Å C24-C28 is 1.452 Å, C24-C25 is 1.3864 Å, and C27-C28 is 1.4155 Å. Other bond length data are also having great agreement with the structure of the title compound. The bond angle of C2-C1-C6 is 118.5673°, N35-C27-C37 is 167.6792°, C25-N35-H36 is 124.8482°, C27-N35-H36 is 125.3017°, C27-C37-C29 is 61.6042°, and C27-C37-C33 is 59.6078°. Similar to bond lengths, bond angles are also in great agreement.

Table 1. Optimized bond length data of ITHF molecule by DFT/ B3LYP with 6-311G(d,p) basis set

Bond lengths (Å)			
C1-C2	1.3995	C17-H19	1.098
C1-C6	1.3938	C17-C21	1.512
C1-H7	1.083	C21-C22	1.3489
C2-C3	1.3911	C22-H23	1.0882
C2-H8	1.0851	C22-C24	1.4399
C3-C4	1.403	C24-C25	1.3864
C3-C17	1.5182	C24-C28	1.452
C4-C5	1.3876	C25-H26	1.0768
C4-C16	1.4832	C25-N35	1.3701
C5-C6	1.3922	C27-C28	1.4155
C5-C9	1.5073	C27-C31	1.3957
C6-O15	1.3631	C27-N35	1.3836
C9-H10	1.0948	C28-C29	1.4021
C9-H11	1.0907	C29-H30	1.084
C9-C12	1.5464	C29-C37	1.3869
C12-H13	1.0941	C31-H32	1.0844
C12-H14	1.0894	C31-C33	1.3873
C12-O15	1.4577	C33-H34	1.0839
C16-O20	1.2207	C33-C37	1.4072
C16-C21	1.4901	N35-H36	1.0064
C17-H18	1.098	C37-H38	1.0838

Table 2. Optimized bond angle data of ITHF molecule by DFT/ B3LYP with 6-311G(d,p) basis set

Bond Angles (°)					
C2-C1-C6	118.5673	H13-C12-O15	107.5001	C31-C27-H38	61.6271
C2-C1-H7	121.3799	H14-C12-O15	107.3392	N35-C27-C37	167.6792
C6-C1-H7	120.0528	C6-O15-C12	107.2649	N35-C27-H38	168.0208
C1 -C2 -C3	119.9549	C4-C16-C20	126.6805	C24-C28-C27	107.4531
C1-C2-H8	119.3584	C4-C16-C21	106.1319	C24-C28-C29	133.7828
C3-C2-H8	120.6859	C20-C16-C21	127.1875	C24-C28-H38	154.996
C2-C3-C4	120.2934	C3-C17-H18	111.5069	C27-C28-C29	118.7641
C2-C3-C17	128.96	C3-C17-H19	111.4606	C29-C28-H38	21.2132
C4-C3-C17	110.7464	C3-C17-H21	103.6253	C28-C29-H30	120.6995
C3-C4-C5	120.4689	H18-C17-H19	106.758	H30-C29-C37	120.3352
C3-C4-C16	110.0855	H18-C17-C21	111.7852	C27-C31-H32	121.514
C5-C4-C16	129.4445	H19-C17-C21	111.8102	C27-C31-C33	117.2802
C4-C5-C6	118.3685	C16-C21-C17	109.4108	H32-C31-C33	121.2059
C4-C5-C9	133.0982	C16-C21-22	120.6638	C31-C33-H34	119.4336
C6-C5-C9	108.4745	C17-C21-C22	129.9254	C31-C33-C37	121.1434
C1-C6-C5	122.345	C21-C22-H23	114.2765	H34-C33-C37	119.4231
C1-C6-O15	124.3887	C21-C22-C24	129.8936	C25-N-35-C27	109.85
C5-C6-C15	113.265	H23-C22-C24	115.8299	C25-N35-H36	124.8482
C5-C9-H10	110.6161	C22-C24-C25	129.2666	C27-N35-H36	125.3017
C5-C9-H11	113.0881	C22-C24-C28	124.9501	C27-C37-C29	61.6042
C5-C9-C12	101.1004	C25-C24-C28	105.7833	C27-C37-C33	59.6078
H10-C9-H11	107.0815	C24-C25-H26	129.934	C28-C37-C33	90.5111
C10-C9-C12	112.2447	C24-C25-N35	109.9007	C29-C37-C33	121.212
H11-C9-C12	112.7689	H26-C25-N35	120.1653	C29-C37-H38	119.6058
C9-C12-H13	111.5569	C28-C27-C31	122.635	C33-C37-H38	119.1822
C9-C12-H14	114.0455	C28-C27-N35	107.0129	-	-
C9-C12-O15	106.9839	C31-C27-N35	130.3521	-	-
H1-C12-H14	109.1082	C31-C27-C37	61.9687	-	-

Mulliken Charge Study

Mulliken nuclear charges are computed employing electron density. The charge distribution on molecules plays a crucial role in quantum mechanical computations for molecular structures. Figure 3 displays a pictorial

representation of the **ITHF** molecule's Mulliken atomic charges as calculated by the DFT/B3LYP strategy with a 6-311G(d,p) base collection, which are tabulated in Table 3. According to Mulliken atomic charges, all hydrogen atoms have a net positive charge, but the H36 hydrogen atom, with an atomic charge of 0.231206, is extremely electropositive. This can be explained by the presence of a nitrogen atom. Of all carbon atoms, the C6 atom has the largest net positive charge (0.238011), while the C21 atom has the highest net negative charge (-0.223465).

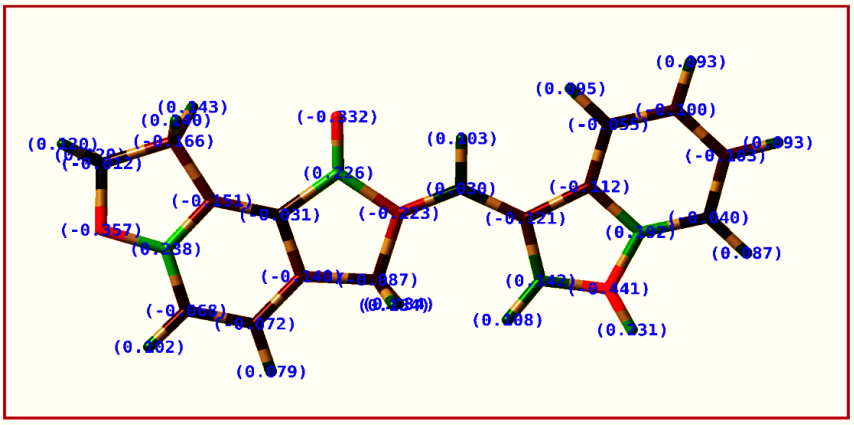

Figure 3. Mulliken atomic charges of ITHF molecule

Table 3. Mulliken atomic charges of ITHF molecule

Atom	Charge	Atom	Charge
1 C	-0.067941	20 O	-0.331903
2 C	-0.072073	21 C	-0.223465
3 C	-0.139505	22 C	0.030134
4 C	-0.030881	23 H	0.102743
5 C	-0.151155	24 C	-0.121282
6 C	0.238011	25 C	0.142017
7 H	0.102130	26 H	0.108385
8 H	0.078968	27 C	0.192375
9 C	-0.166374	28 C	-0.111941
10 H	0.139746	29 C	-0.055485
11 H	0.143308	30 H	0.095022
12 C	-0.012196	31 C	-0.039770
13 H	0.120070	32 H	0.087005
14 H	0.120365	33 C	-0.102738
15 O	-0.357419	34 H	0.093166
16 C	0.226458	35 N	-0.441363
17 C	-0.086756	36 H	0.231206
18 H	0.134046	37 C	-0.100405
19 H	0.134094	38 H	0.093401

Molecular Electrostatic Surface Potential (MESP) Study

The MESP plot of **ITHF** is shown in Figure 4. The MESP guide can be used to relate any molecule's properties such as dipole moment, electronegativity, partial charges, and chemical reactivity. The molecular electrostatic potential is the total charge distribution of a molecule space. Different coloured areas reflect positive, negative, and neutral potentials. It can be shown that negative electrostatic potential occurs over oxygen atoms in this situation. The positive electrostatic potential, on the other hand, is located over two aromatic rings' hydrogen atoms. The zones with varying electrostatic potential are likely to provide important knowledge about multiple types of intermolecular interactions, allowing one to predict the molecule's chemical behaviour.

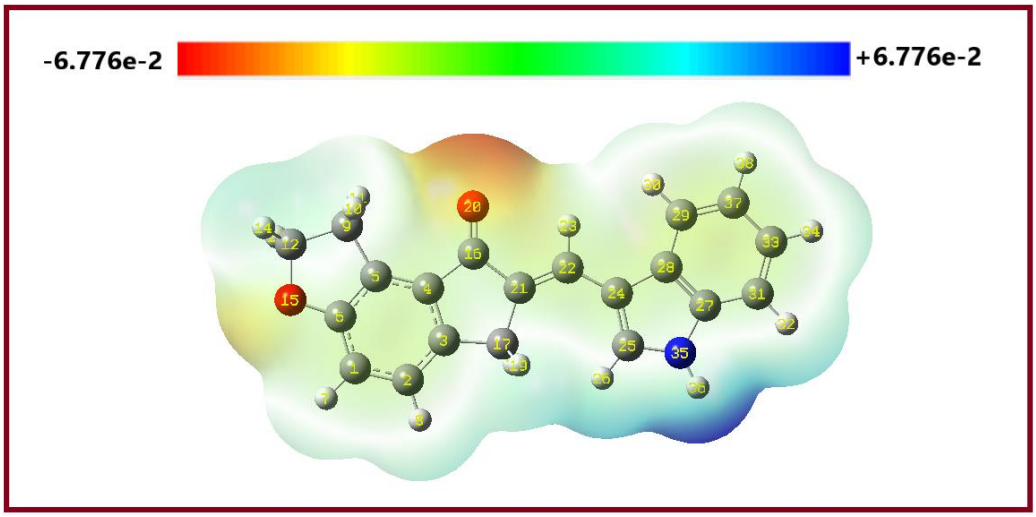

Figure 4. Molecular electrostatic surface potential of ITHF molecule

Frontier Molecular Orbital Study

The HOMO-LUMO analysis is often used to forecast the most receptive condition in -electron frameworks and to describe a few forms of conjugated mechanism responses [66-71]. A smaller HOMO-LUMO energy difference indicates a weaker molecule, while a large gap indicates a harder molecule. The knowledge about charge transfer within the molecule can be envisioned using the frontier molecular orbital (FMO) investigation. Figure 5 depicts the **ITHF** molecule's maximum inhabited molecular orbital (HOMO) and lowest unoccupied molecular orbital (LUMO). The bioactive property of the molecule is based on the charge transfer phenomenon. The FMO thesis elucidates the molecule's reactivity, and the active site can be determined by the distribution of frontier orbitals. The HOMO and LUMO parameters are important in the analysis of quantum chemical parameters. The HOMO-LUMO analysis is often used to forecast the most receptive condition in electron frameworks and to describe a few forms of conjugated mechanism responses. A smaller HOMO-LUMO energy difference indicates a weaker molecule, while a large gap indicates a harder molecule. In **ITHF**, the HOMO-LUMO energy difference is 3.67 eV.

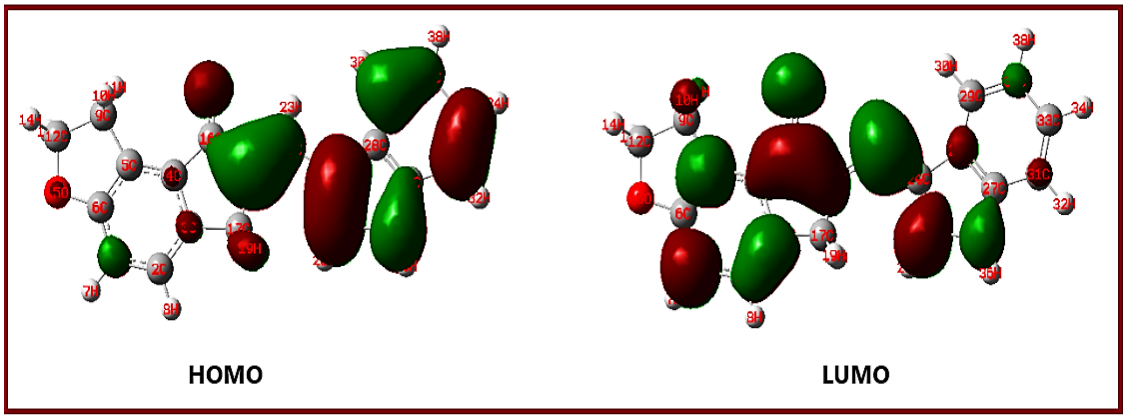

Figure 5. HOMO-LUMO pictures of ITHF molecule

Antimicrobial Screening Study

The antibacterial activity of the synthesised compound **ITHF** was examined on two Gram positive and two Gram negative bacteria, while the antifungal activity was tested on two fungal species. Table 4 summarises the findings of the antimicrobial evaluation. According to the observations, the **ITHF** is a mild antimicrobial agent against the strains examined. The findings have showed that **ITHF** is a more antibacterial than antifungal agent, with stronger antibacterial activity than antifungal activity. The **ITHF** has not been found to be successful against *Staphylococcus aureus* Gram strain among the strains examined. The **ITHF** compound has been identified to be a more effective antibacterial agent than an antifungal agent. The antimicrobial information provided here may indeed be a good approach for further antimicrobial agent research.

Table 4. Zone of inhibition shown by ITHF against four bacterial and two fungal agents

Entry	*E.* coli	*P.* vulgaris	*S.* aureus	*B.* subtilis	*A.* niger	*C.* albicans
ITHG	++	++	_	++	-	+
Chloramphenicol	+++++	+++++	+++++	+++++	NA	NA
Amphotericin-B	NA	NA	NA	NA	++++	++++

+ = < 5 mm zone, ++ = 5-10 mm zone, +++ = >10-15 mm zone, ++++ = >15-20 mm, +++++ = > 20 mm, - = No inhibition, NA = Not applicable

Conclusions

In summary, the present investigation covers the synthesis, antibacterial, antifungal, and computational aspects of (*E*)-7-((1*H*-indol-3-yl)methylene)-1,2,6,7-tetrahydro-8*H*-indeno[5,4-*b*]furan-8-one. The ^{1}H NMR and ^{13}C NMR spectral techniques were used to affirm the structure of the titled compound. The DFT examination used the Becke-3-Lee-Yang-Parr functional (B3LYP) level of theory at the 6-311G(d,p) basis set. The **ITHF** molecule has C1 point group symmetry. The optimized geometrical parameters bond lengths and bond angles are also described. All hydrogen atoms have a net positive charge, the C6 atom has the highest net positive charge and the C21 atom has the highest net negative charge in the titled compound. It can be seen from MESP that, negative electrostatic potential exists over oxygen atoms. The HOMO-LUMO energy gap in **ITHF** is 3.67 eV. The antimicrobial screening against bacterial and fungal strains revealed here

that the **ITHF** compound is a more effective antibacterial agent than an antifungal agent.

Acknowledgement

The author acknowledges the central instrumentation facility (CIF), Savitribai Phule Pune University, Pune for the spectral analysis. The author is very much thankful to Prin. Dr. B.S. Jagdale for providing necessary research facilities. The author is grateful to Professor Dr. A. B. Sawant and Professor Dr. T.B. Pawar for the Gaussian study. Dr. Aapoorva P. Hiray Coordinator, M. G. Vidyamandir institute is gratefully acknowledged for the Gaussian package.

Disclosure statement

No potential conflict of interest was reported by the author.

ORCID

Vishnu Ashok Adole **:** 0000-0001-7691-7884

References

[1] S. Biswal, U. Sahoo, S. Sethy, H.K.S. Kumar, M. Banerjee, *Asian J. Pharm. Clin. Res.*, **2012**, *5*, 1–6. [Google Scholar], [Publisher]

[2] N.K. Kaushik, N. Kaushik, P. Attri, N. Kumar, C.H. Kim, A.K. Verma, E.H. Choi, *Molecules*, **2013**, *18*, 6620–6662. [CrossRef], [Google Scholar], [Publisher]

[3] Y. Wan, Y. Li, C. Yan, M. Yan, Z. Tang, *Eur. J. Med. Chem.*, **2019**, *183*, 111691. [CrossRef], [Google Scholar], [Publisher]

[4] T.V Sravanthi. S.L. Manju, *Eur. J. Pharm. Sci.*, **2016**, *91*, 1–10. [CrossRef], [Google Scholar], [Publisher]

[5] M. Sayed, A.M. Kamal El-Dean, M. Ahmed, R. Hassanien, *Synth. Commun.*, **2018**, *48*, 413–421. [CrossRef], [Google Scholar], [Publisher]

[6] S.V. Karthikeyan, S. Perumal, K.A. Shetty, P. Yogeeswari, D. Sriram, *Bioorganic Med. Chem. Lett.*, **2009**, *19*, 3006–3009. [CrossRef], [Google Scholar], [Publisher]

[7] P. Ahuja, N. Siddiqui, *Eur. J. Med. Chem.*, **2014**, *80*, 509–522. [CrossRef], [Google Scholar], [Publisher]

[8] A.S.H. da Silva Guerra, D.J. do Nascimento Malta, L.P.M. Laranjeira, M.B.S. Colaço, N.C. Maia, M.D.C.A. de Lima, S.L. Galdino, I. da Rocha Pitta, T. Gonçalves-Silva, *Int. Immunopharmacol.*, **2011**, *11*, 1816–1822. [CrossRef], [Google Scholar], [Publisher]

[9] M.A. Radwan, E.A. Ragab, N.M. Sabry, S.M., El-Shenawy, *Bioorg. Med. Chem.*, **2007**, *15*, 3832–3841. [CrossRef], [Google Scholar], [Publisher]

[10] J. Singh Sidhu, R. Singla, V. Jaitak, *Anticancer Agents Med. Chem.*, **2016**, *16*, 160–173. [CrossRef], [Google Scholar], [Publisher]

[11] H. Hayashi, K. Takiuchi, S. Murao, M. Arai, *Agricultural and biological chemistry*, **1989**, *53*, 461–469. [CrossRef], [Google Scholar], [Publisher]

[12] M.S. Estevão, L.C. Carvalho, D. Ribeiro, D. Couto, M. Freitas, A. Gomes, L.M. Ferreira, E. Fernandes, M.M.B. Marques, *Eur. J. Med. Chem.*, **2010**, *45*, 4869–4878. [CrossRef], [Google Scholar], [Publisher]

[13] M.Z. Zhang, Q. Chen, G.F. Yang, *Eur. J. Med. Chem.*, **2015**, *89*, 421–441. [CrossRef], [Google Scholar], [Publisher]

[14] P.O. Patil, S.B. Bari, *Arab. J. Chem.*, **2016**, *9*, 588–595. [CrossRef], [Google Scholar], [Publisher]

[15] M. Ajitha, K. Rajnarayana, M. Sarangapani, *Pharmazie*, **2002**, *57*, 796–799. [Google Scholar]

[16] V.A. Adole, T.B. Pawar, B.S. Jagdale, *J. Chin. Chem. Soc.*, **2020**, *67*, 306–315. [CrossRef], [Google Scholar], [Publisher]

[17] P. Rajagopalan, K.A. Alahmari, A.A. Elbessoumy, M. Balasubramaniam, R. Suresh, M.E.A. Shariff, H.C. Chandramoorthy, *Cancer Chemother. Pharmacol.*, **2016**, *77*, 393–404. [CrossRef], [Google Scholar], [Publisher]

[18] J.C. Menezes, *RSC adv.*, **2017**, *7*, 9357–9372. [CrossRef], [Google Scholar], [Publisher]

[19] M. Turek, D. Szczęsna, M. Koprowski, P. Bałczewski, *Beilstein J. Org. Chem.*, **2017**, *13*, 451–494. [CrossRef], [Google Scholar], [Publisher]

[20] P. Rajagopalan, H.C. Chandramoorthy, *Asian Biomed.*, **2020**, *13*, 131–139. [CrossRef], [Google Scholar], [Publisher]

[21] V.A. Adole, T.B. Pawar, B.S. Jagdale, *J. Sulphur Chem.*, **2021**, *42*, 131–148. [CrossRef], [Google Scholar], [Publisher]

[22] V.A. Adole, R.H. Waghchaure, S.S. Pathade, M.R. Patil, T.B. Pawar, B.S. Jagdale, *Mol. Simul.*, **2020**, *46*, 1045–1054. [CrossRef], [Google Scholar], [Publisher]

[23] S.L. Dhonnar, V.A. Adole, N.V. Sadgir, B.S. Jagdale, *Phys. Chem. Res.*, **2021**, *9*, 193–209. [CrossRef], [Google Scholar], [Publisher]

[24] S.S. Pathade, B.S. Jagdale, *Phys. Chem. Res.*, **2020**, *8*, 671–687. [CrossRef], [Google Scholar], [Publisher]

[25] M. Shkir, S. AlFaify, H. Abbas, S. Muhammad, *Spectrochim. Acta A,* **2015**, *147*, 84–92. [CrossRef], [Google Scholar], [Publisher]

[26] A. Srivastava, R. Mishra, S. Kumar, K. Dev, P. Tandon, R. Maurya, *J. Mol. Struct.,* **2015**, *1084*, 55–73. [CrossRef], [Google Scholar], [Publisher]

[27] P. Manjusha, S. Muthu, B.R. Raajaraman, *J. Mol. Struct.*, **2020**, *1203*, p.127394. [CrossRef], [Google Scholar], [Publisher]

[28] A. Kumer, M.J. Islam, S. Paul, *Chem. Methodol.*, **2020**, *4*, 595–604. [CrossRef], [Google Scholar], [Publisher]

[29] A. Kumer, N. Sarker, S. Paul, A. Zannat, *Adv. J. Chem. A,* **2019**, *2*, 190–202. [Google Scholar], [Publisher]

[30] A. Kumer, M.N. Sarker, P.A.U.L. Sunanda, *Int. J. Chem. Technol.*, **2019**, *3*, 26–37. [CrossRef], [Google Scholar], [Publisher]

[31] M.J. Islam, A. Kumer, N. Sarker, S. Paul, A. Zannat, *Adv. J. Chem. A,* **2019**, *2*, 316–326. [Google Scholar], [Publisher]

[32] J.R. Hidalgo, A. Neske, M.A. Iramain, P.E. Alvarez, P.L. Bongiorno, S.A. Brandán, *J. Mol. Struct.*, **2019**, *1196*, 508–517. [CrossRef], [Google Scholar], [Publisher]

[33] M. Raja, R.R. Muhamed, S. Muthu, M. Suresh, *J. Mol. Struct.*, **2017**, *1141*, 284–298. [CrossRef], [Google Scholar], [Publisher]

[34] M.A. Iramain, L. Davies, S.A. Brandán, *J. Mol. Struct.*, **2018**, *1158*, 245–254. [CrossRef], [Google Scholar], [Publisher]

[35] A. Nath, A. Kumer, M.W. Khan, *J. Mol. Struct.*, **2021**, *1224*, 129225. [CrossRef], [Google Scholar], [Publisher]

[36] M.M. Hoque, M.S. Hussen, A. Kumer, M.W. Khan, *Mol. Simul.*, **2020**, *46*, 1298–1307. [CrossRef], [Google Scholar], [Publisher]

[37] A. Kumer, M.N. Sarker, S. Paul, *Turkish Comp. Theo. Chem.*, **2019**, *3*, 59–68. [CrossRef], [Google Scholar], [Publisher]

[38] R.A. Shinde, V.A. Adole, B.S. Jagdale, T.B. Pawar, B.S. Desale, R.S. Shinde, *Mat. Sci. Res. India,* **2020**, *17,* 146–161. [CrossRef], [Google Scholar], [Publisher]

[39] S.S. Pathade, B.S. Jagdale, *J. Adv. Sci. Res.*, **2020**, *11*, 87–94. [Google Scholar]

[40] V.A. Adole, P.B. Koli, R.A. Shinde, R.S. Shinde, *Mat. Sci. Res. India,* **2020,** *17*, 41–53. [CrossRef], [Google Scholar], [Publisher]

[41] V.A. Adole, R.H. Waghchaure, B.S. Jagdale, T.B. Pawar, *Chem. Bio. Interface*, **2020**, *10*, 22–30. [Google Scholar]

[42] S.S. Pathade, V.A. Adole, B.S. Jagdale, T.B. Pawar, *Mat. Sci. Res. India*, **2020**, *17*, 27–40. [CrossRef], [Google Scholar], [Publisher]

[43] R.A. Shinde, V.A. Adole, B.S. Jagdale, T.B. Pawar, *Mat. Sci. Res. India*, **2020**, *17,* 54–72. [CrossRef], [Google Scholar], [Publisher]

[44] A.R. Bukane, B.S. Jagdale, *J. Adv. Chem. Sci.*, **2021**, *7*, 717–720 [CrossRef], [Google Scholar]

[45] N.V. Sadgir, S.L. Dhonnar, B. Jagdale, B. Waghmare, C. Sadgir, *Mat. Sci. Res. India*, **2020**, *17*, 281–293. [CrossRef], [Google Scholar], [Publisher]

[46] V.A. Adole, B.S. Jagdale, T.B. Pawar, B.S. Desale, *Mat. Sci. Res. India*, **2020**, *17*, 13–36. [CrossRef], [Google Scholar], [Publisher]

[47] V.A. Adole, T.B. Pawar, P.B. Koli, B.S. Jagdale, *J. Nanostructure Chem.*, **2019**, *9*, 61–76. [CrossRef], [Google Scholar], [Publisher]

[48] V.A. Adole, R.A. More, B.S. Jagdale, T.B. Pawar, S.S. Chobe, *ChemistrySelect*, **2020**, *5*, 2778–2786. [CrossRef], [Google Scholar], [Publisher]

[49] R.H. Waghchaure, T.B. Pawar, *World J. Pharm. Res.*, **2020**, *9*, 1867–1881. [Google Scholar], [Publisher]

[50] V.A. Adole, B.S. Jagdale, T.B. Pawar, A.A. Sagane, *S. Afr. J. Chem.*, **2020**, *73*, 35–43. [CrossRef], [Google Scholar], [Publisher]

[51] B.S. Jagdale, S.S. Pathade, *J. Appl. Chem.*, **2019**, *8*, 12–19. [Google Scholar]

[52] S.S. Chobe, V.A. Adole, K.P. Deshmukh, T.B. Pawar, B.S. Jagdale, *Arch. Appl. Sci. Res.*, *6*, 61–66. [Google Scholar]

[53] V.A. Adole, *World J. Pharm. Res.*, **2020**, *9*, 1067–1091. [Google Scholar]

[54] N.V. Sadgir, S.L. Dhonnar, B.S. Jagdale, A.B. Sawant, *SN Appl. Sci.*, **2020**, *2*, 1–12. [CrossRef], [Google Scholar], [Publisher]

[55] R. Basri, M. Khalid, Z. Shafiq, M.S. Tahir, M.U. Khan, M.N. Tahir, M.M. Naseer, A.A.C. Braga, *ACS omega*, **2020**, *5*, 30176–30188. [CrossRef], [Google Scholar], [Publisher]

[56] N.V. Sadgir, S.L. Dhonnar, B.S. Jagdale, B. Waghmare, C. Sadgir, *Mat. Sci. Res. India,* **2020**, *17*, 281–293. [CrossRef], [Google Scholar], [Publisher]

[57] R. Bhuvaneswari, M.D. Bharathi, G. Anbalagan, G. Chakkaravarthi, K.S. Murugesan, *J. Mol. Struct.*, **2018**, *1173*, 188–195. [CrossRef], [Google Scholar], [Publisher]

[58] R.A. Shinde, V.A. Adole, *J. Appl. Organomet. Chem.*, **2021**, *1*, 48–58. [CrossRef], [Publisher]

[59] D. Pegu, J. Deb, S.K. Saha, M.K. Paul, U. Sarkar, *J. Mol. Struct.*, **2018**, *1160*, 167–176. [CrossRef], [Google Scholar], [Publisher]

[60] V.A. Adole, B.S. Jagdale, T.B. Pawar, A.B. Sawant, *J. Chin. Chem. Soc.*, **2020**, *67*, 1763–1777. [CrossRef], [Google Scholar], [Publisher]

[61] S.L. Dhonnar, B.S. Jagdale, A.B. Sawant, T.B. Pawar, S.S. Chobe, *Der Pharma Chem*, **2016**, *8*, 119–128. [Google Scholar]

[62] V.A. Adole, V.R. Bagul, S.A. Ahire, R.K. Pawar, G.B. Yelmame, A.R. Bukane, *J. Adv. Sci. Res.,* **2021**, *12*, 276–286. [Google Scholar]

[63] M.J. Frisch, "Gaussian 03, revision C. 02; Gaussian, Inc.: Wallingford, CT, **2004**. [Google Scholar], [Publisher]

[64] (a) A.D. Becke, *J. Chem. Phys.*, **1993**, *98*, 5648–5652. [CrossRef], [Google Scholar]; (b) A.D. Becke, *J. Chem. Phys.*, **1993**, *98*, 1372–1377. [CrossRef], [Google Scholar]

[65] (a) J.H. Jorgensen, J.D. Turnidge *Manual of Clinical Microbiology*, Eleventh Edition: American Society of Microbiology, **2015**, p 1253. [CrossRef], [Google Scholar], [Publisher]; (b) E.M. Johnson, M. Cavling-Arendrup, *Manual of Clinical Microbiology*, Eleventh Edition American Society of Microbiology, **2015**, p. 2255. [CrossRef], [Google Scholar], [Publisher]

[66] A. Kumer, M.N. Sarker, P.A.U.L. Sunanda, *Eurasian J. Environ. Res.,* **2019**, *3*, 1–10. [Google Scholar], [Publisher]

[67] M.N. Sarker, A. Kumer, M.J. Islam, S. Paul, *Asian J. Nanosci. Mater.*, **2019**, *2*, 439–447. [CrossRef], [Google Scholar], [Publisher]

[68] M.K. Ahmed, A. Kumer, A.B. Imran, *R. Soc. Open Sci.*, **2021**, *8*, 202056. [CrossRef], [Google Scholar], [Publisher]

[69] V.A. Adole, *J. Appl. Organomet. Chem.*, **2021**, *1*, 29–40. [CrossRef], [Publisher],

[70] T.B. Pawar, B.S. Jagdale, A.B. Sawant, V.A. Adole, *J. Chem. Biol. Phys. Sci.*, **2017,** *7*, 167–175. [Google Scholar]

[71] V.A. Adole, R.H. Waghchaure, T.B. Pawar, B.S. Jagdale, K.H. Kapadnis, *Asian J. Org. Med. Chem.*, **2020**, 242–248. [CrossRef], [Google Scholar], [Publisher]

HOW TO CITE THIS ARTICLE Vishnu Ashok Adole*, Synthesis, Antibacterial, Antifungal and DFT Studies on Structural, Electronic and Chemical Reactivity of (*E*)-7-((1*H*-Indol-3-yl)methylene)-1,2,6,7-tetrahydro-8*H*-indeno[5,4-*b*]furan-8-one. *Adv. J. Chem. A*, **2021**, 4(3), 175-187.
DOI: 10.22034/AJCA.2021.278047.1250 **URL:** http://www.ajchem-a.com/article_129397.html